earlier study (23). In addition, it has not yet been fully clarified in which pathological conditions or in which types of disease this protein is implicated, although available evidence suggests that Prx-4 plays a role in ER stress and the oxidative folding of proteins in the ER (24,25). To extend the clinical usefulness of Prx-4, a more quantitative assay is required to determine and compare Prx-4 levels in various mammalian tissues.

In this study, we report on the preparation of a specific polyclonal antibody by immunization of a rabbit with a purified recombinant Prx-4, which was previously described (26). An enzyme-linked immunosorbent assay (ELISA) was then developed to quantitatively determine its levels in tissues and to investigate alterations of its levels in association with certain pathological conditions using animal models. The findings suggest that the serum level of Prx-4 is associated with the pathological state of the liver and may be of potential value for monitoring oxidative stress in the liver.

Materials and methods

Cell culture. The rat cell lines used in this study were maintained at 37°C in RPMI-1640 (AH66 cells), Eagle's MEM (WB-F344 and RLN-10 cells) and DMEM (RLC-16 cells), all of which were supplemented with 5 or 10% fetal bovine serum, streptomycin and penicillin, under an atmosphere of 5% CO_2 in humidified air.

Animals. Male Wistar rats were purchased from Japan SLC Inc. (Hamamatsu, Japan) at the age of 6 weeks, and Long-Evans Cinnamon (LEC) rats and Sprague-Dawley (SD) rats were obtained at the age of 18 weeks from Charles River Japan, Inc. (Yokohama, Japan). The rats were maintained under specific pathogen-free conditions at a constant temperature of 20-22°C with a 12-h light/dark cycle. The Wister rats were injected with a single dose of 50 mg/kg streptozotocin (Sigma) to induce diabetes. In the LEC rats, serum alanine transaminase (ALT) and aspartate transaminase (AST) activities were determined using a transaminase assay kit (Wako Pure Chemicals) to verify the occurrence of hepatitis. Animal handling and care were conducted under the protocol approved by the Institutional Animal Research Committee of Saga University.

Expression and purification of recombinant rat Prx-4. Preparation of the recombinant Prx-4 protein was conducted as previously described (26). The recombinant protein was obtained from the extract of the Sf21 cells that had been infected with a recombinant baculovirus encoding a signal peptide-truncated form of rat Prx-4. The enzyme was purified by two successive cation exchanges and gel filtration column chromatographies, following polyethyleneimine precipitation. As previously described (26), the recombinant protein was enzymatically active and homogeneous.

Preparation and biotinylation of rabbit anti-Prx-4 IgG. A total of 500 μg of the purified rat Prx-4 was emulsified in Freund's complete adjuvant and injected intracutaneously into the dorsal skin of a female rabbit. Another 500 μg of protein in incomplete adjuvant were subcutaneously injected dorsally at two-week intervals. Antiserum was obtained three weeks after the final booster injection. The IgG fraction was prepared from the antiserum by ammonium sulfate precipitation and subsequent column chromatography using Protein A Sepharose Fast Flow (GE Healthcare). Biotinylation of the antibody was conducted using N-hydroxysuccinimide-biotin (Pierce), according to the manufacturer's instructions.

Electrophoresis and immunoblot analysis. After the protein samples were separated using sodium dodecyl sulfate-polyacrylamide gel electrophoresis (SDS-PAGE), they were electrophoretically transferred onto a polyvinylidene fluoride membrane (Millipore). The membrane was blocked by treatment with 1% skimmed milk in phosphate-buffered saline (PBS) and reacted with the polyclonal rabbit antibody. After washing, the membrane was incubated with a horseradish peroxidase-conjugated antibody against rabbit IgG. Following washing, the reactive protein bands were visualized using an ECL Advance Western Blotting Detection kit (Amersham).

ELISA. The 96-well microtiter plates (Maxisorp, Nunc) were pre-coated with rabbit polyclonal IgG against rat Prx-4. The IgG solution was diluted in 50 mM $NaHCO_3$ (pH 9.6) to 50 μg/ml and added to the wells. The plates were incubated overnight at 4°C and were then blocked by 1% bovine serum albumin (BSA) after washing with PBS. A total of 50 μl of the appropriately diluted samples were added in duplicate to the wells of the plates, followed by incubation at room temperature for 2 h. Biotinylated anti-rat Prx-4 rabbit IgG was added to the plates, and the plates were then allowed to react at room temperature for 1 h. The plates were then incubated at room temperature for 30 min after adding horseradish peroxidase-conjugated streptavidin to the wells. The plates were washed five times with PBS-Tween-20 (PBS-T) after each step. Detection was performed using a solution of 1 mg/ml *o*-phenylenediamine as the substrate with 0.015% H_2O_2 in 0.1 M citrate-phosphate buffer (pH 5.4). The absorbance at 490 nm was measured using a microtiter plate reader (Bio-Rad).

Tissue sample preparation for immunoblot analysis and ELISA. The rats were sacrificed after appropriate periods of time, and then the tissues were obtained and stored at -80°C until use. The tissues were homogenized with a Dounce homogenizer in a lysis buffer of 20 mM Tris-HCl, 150 mM NaCl, 5 mM EDTA, 1% (v/v) Nonidet P-40, 10% (v/v) glycerol, 1 mM phenylmethylsulfonyl fluoride, 2 μg/ml aprotinin and 5 μg/ml leupeptin (pH 7.4)

Protein determination. Protein contents were determined using a Bradford protein assay kit (Pierce). BSA was used as the standard.

Statistical analysis. Data were analyzed using the t-test and the results are expressed as the means ± standard deviation (SD). $P<0.05$ was considered to indicate a statistically significant difference, unless otherwise stated.

Results

Antibody raised against native Prx-4 protein. In earlier studies, specific antibodies have been prepared using an

inactive denatured polypeptide or a synthetic polypeptide as the antigen (21,23,27). The use of the native form of a protein can occassionally prove more benificial for immunization. For example, when an antibody that effectively recognizes a native protein is desired, the latter is recommended. Thus, the enzymatically active recombinant Prx-4 was purified and used as the antigen to immunize rabbits in this study. The anti-Prx-4 IgG was purified from antiserum obtained from the immunized rabbits. The specificity of the antibody was verified using immunoblot analysis of several rat tissues (Fig. 1). All samples examined displayed identical protein bands corresponding to a signal peptide-processed form, with the exception of the testis; consistent with a previous study using a different antibody which was raised against a bacterially produced antigen (21,27). No other bands that could correspond to other Prx isoforms with different molecular masses were detected, thus indicating that the specificity of this antibody was sufficient. The results were in accordance with data reported in a previous study, and demonstrated that the protein levels of Prx-4 were relatively higher in the testis, pancreas and liver.

ELISA for Prx-4 and examination of tissue distribution. Although in a previous study, we examined tissue distribution of Prx-4 in rats, the protein levels were roughly estimated by immunoblot analysis (21). In order to more quantitatively estimate the levels of Prx-4 in tissues, we developed an ELISA using the aforementioned antibody. This ELISA involved the immobilized antibody, the biotin-labeled antibody and HRP-conjugated streptavidin, as described in detail in the Materials and methods section. A typical calibration curve for the standard samples is shown in Fig. 2A. As indicated, this assay enabled us to optimally estimate the levels in the range between 0.1 and 10 ng/ml. The re-assessment of the tissue distribution using ELISA was essentially consistent with the results obtained by the immunoblot analyses, as described above, as well as in the previous study. As shown for normal control rats in Fig. 2B, the expression of Prx-4 was significantly higher in the pancreas, liver and testis. The higher expression of Prx-4 in the pancreas and liver may be associated with the possible role of this protein in the oxidative folding of secretory proteins in the ER.

Prx-4 levels in the tissues of streptozotocin-induced diabetic rats. The issue of whether or not Prx-4 is implicated in diseases of the pancreas and liver has not yet been fully investigated; thus we examined the levels of Prx-4 in certain pathological states using animal models. Eight-week-old Wistar rats were treated with streptozotocin to induce severe diabetes. The occurrence of the disease was verified by high blood sugar levels and the production of urinary sugar. Measurements of blood sugar indicated levels of 130±35 and 440±67 mg/dl for the control rats and streptozotocin-treated rats, respectively (P<0.01, t-test; n=3 for each group). The protein levels of Prx-4 were determined by ELISA in various tissues of the control and diabetic rats. As shown in Fig. 2B, although a slight decrease in the Prx-4 level was observed in the liver and pancreas, there was no statistically significant difference in all tissues examined. The mean serum level values of the proteins were estimated to be 1.7 and 2.2 ng/ml in normal and diabetic rats, respectively. However, a statistical analysis indicated no
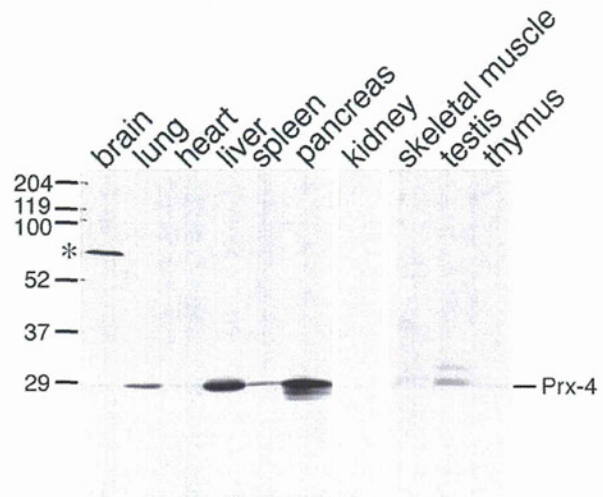

Figure 1. Immunoblot analysis of rat tissues with anti-rat Prx-4 antibody. A total of 50 μg of proteins from a tissue homogenate were loaded per lane in SDS-PAGE. Data for skeletal muscle, testis and thymus (right three lanes) are presented by a different gel from that of the other data. *Unidentified protein band reactive for the antibody in the immunoblot, possibly due to being denatured, but not detected in the ELISA. Prx, peroxiredoxin; SDS-PAGE, sodium dodecyl sulfate-polyacrylamide gel electrophoresis; ELISA, enzyme-linked immunosorbent assay.
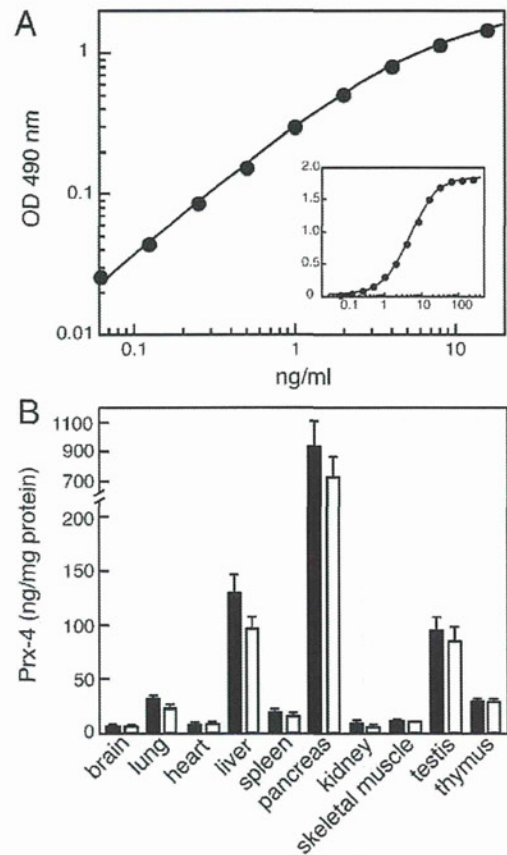

Figure 2. ELISA for rat Prx-4 and tissue distribution in normal and diabetic rats. (A) A linear portion of the standard ELISA curve is shown. Superimposed is the overall standard curve for a wider range. (B) Tissue distribution in normal and streptozotocin-induced diabetic rats. Closed and open columns represent data for normal and diabetic rats, respectively. ELISA, enzyme-linked immunosorbent assay; Prx, peroxiredoxin.
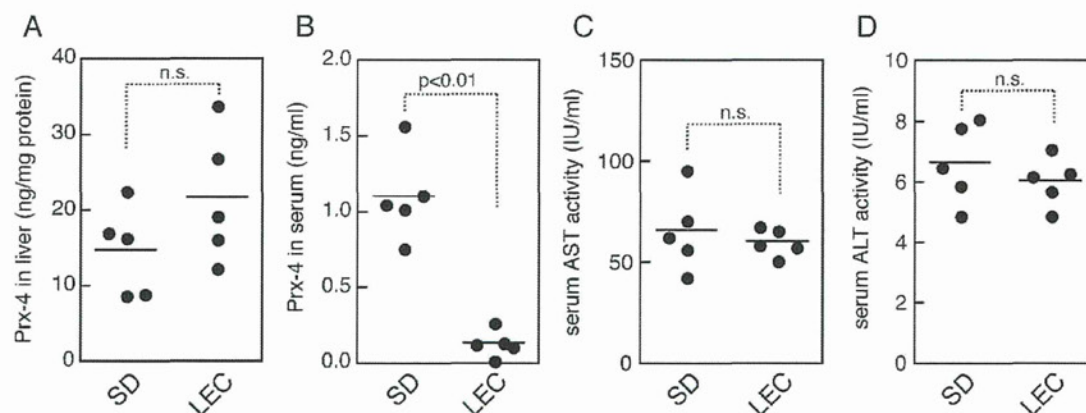
Figure 3. Prx-4 levels and transaminase activities in LEC rats. Levels of Prx-4 in the (A) liver and (B) serum were assayed in LEC rats compared with the control SD rats. Serum transaminase activities of (C) AST and (D) ALT were also determined in the two rat strains. Serum Prx-4 levels are significantly different between LEC and SD rats (P<0.01, n=5 for each group), but no statistical significance was observed for the liver Prx-4 or for serum transaminases. Prx, peroxiredoxin; LEC, Long-Evans Cinammon; SD, Sprage-Dawley; AST, aspartate transaminase; ALT, alanine transaminase.
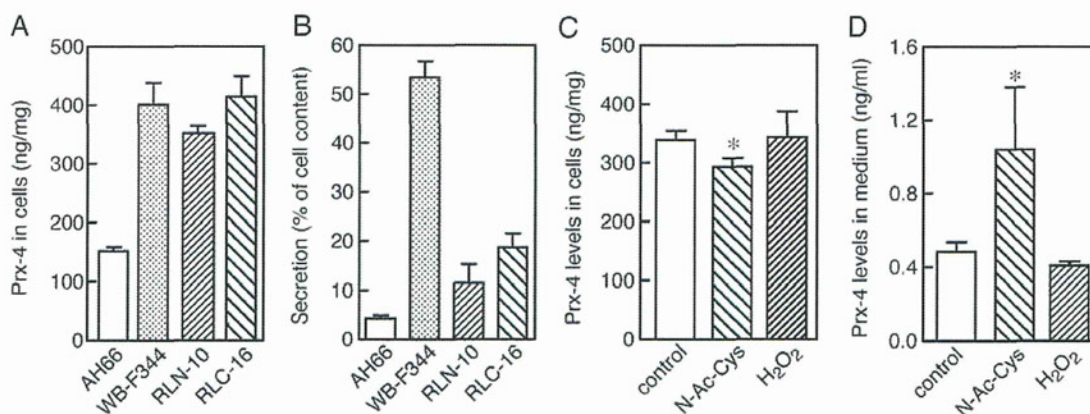

Figure 4. Prx-4 levels in various cell lines derived from rat liver and effects of an oxidant and a reductant on the secretion. (A) Prx-4 contents in cells were determined for various rat cell lines. (B) Secreted Prx-4 was estimated by evaluating the levels in the medium, and the data are expressed as the relative value to the contents in the cells. (C and D) Effects of 0.05 mM H_2O_2 and 5 mM N-acetyl cysteine (N-Ac-Cys) on the secretion of Prx-4 were examined in RLN-10 cells. Prx-4 contents in cells and medium were assayed 24 h after the addition of these agents. *Significant difference compared to controls (P<0.05). Prx, perioxiredoxin.

significant difference despite a tendency toward an increase caused by the streptozotocin treatment.

Alteration of Prx-4 levels in hepatic disease model rats. Another animal model, which has been used for liver disease, is the LEC rats (28). LEC rats are frequently used as a Wilson's disease animal model for which a genetic defect was found in the copper transporter ATPase gene, *Atp7b* (29,30). The rats exhibit abnormal copper accumulation in the liver, and suffer from the development of hepatitis and hepatocarcinogenesis (31). Prx-4 levels were determined in the livers and sera of 24-week-old LEC rats. SD rats of the same age were used as the healthy controls. The LEC rats appeared to be healthy in this study, and did not appear to suffer from hepatitis, as also indicated by ALT and AST assays (Fig. 3C and D). When the serum levels of Prx-4 were determined, however, the data indicated that the levels in the LEC rats were significantly less than those in the normal rats (Fig. 3B). On the other hand, in contrast to the serum levels, LEC rats demonstrated a trend

toward a higher level in the liver, compared to the controls, although no statistically significant difference was observed for Prx-4 levels in the liver (Fig. 3A).

Expression of Prx-4 in rat hepatic cell lines and effects of redox stress on secretion from cells. As suggested by the lower levels of serum Prx-4 in LEC rats, it appeared likely that the redox state affects the release of Prx-4 from the cells since it is well-known that an abnormal accumulation of hepatic copper causes oxidative stress in LEC rats (32,33). Rat hepatic cell lines were used in order to assess whether oxidative stress alters the secretion of Prx-4. Four cell lines, AH66, WB-F344, RLN-10 and RLC-16, were cultured for three days, and the Prx-4 levels in the cells and medium were then separately determined by ELISA. The expression of Prx-4 was observed in all cell lines examined (Fig. 4A). However, the levels of the Prx-4 protein varied in the medium, regardless of the contents associated with the cells, suggesting that the efficiency of secretion varies among the cell lines (Fig. 4B). Only a single

protein band, in which the signal peptide was cleaved off, was observed for all cell lines in the immunoblot analyses (data not shown), suggesting that variations in the extent of secretion are not due to differences in the processing capability of the cells. The difference in secretion appeared to be due to the status or character of the cells rather than to a factor intrinsic to the protein. As observed in RLN-10 cells, treatment with 5 mM N-acetylcysteine for 24 h significantly increased the extent of secretion into the medium, accompanied by a corresponding decrease in the cells. However, the presence of 0.05 mM H_2O_2 did not greatly suppress the secretion of Prx-4 24 h after addition. This discrepancy between the experiments using the reducing and the oxidizing agent may be explained by more intensive oxidative stress in the cells cultured under the condition of 20% O_2 than in the tissues where a partial pressure of O_2 is expected to be lower (34-36). These results suggest that the release of Prx-4 from cells is, at least in part, affected by the redox state of the cells.

Discussion

In this study, we prepared a polyclonal antibody against rat Prx-4 using a purified recombinant protein as the antigen, and subsequently developed an immunoassay for quantitatively determining the levels of the Prx-4 protein. An enzymatic activity assay for thioredoxin-dependent peroxidase cannot be used to specifically evaluate the tissue levels of Prx-4 as the peroxidase activities of the mammalian Prx family are relatively weak; much less than other typical peroxidases, such as glutathione peroxidase. In addition, the enzymatic activity assay does not permit the measurement of each individual member of the Prx family. Therefore, an isoform-specific immunoassay would be useful and desirable for such a quantification in investigations of the role of Prx-4 in various diseases.

The development of the ELISA for Prx-4 confirmed high levels of expression in the pancreas, liver and testis of rats. Considering tissue mass, the total content of Prx-4 is highest in the liver, and thus it is more likely that the supply of the protein to the blood largely depends on the liver. As previously described, Prx-4 appears to be highly expressed in exocrine pancreas rather than islets (37), and another study also reported that another Prx isoform is highly expressed in pancreatic islet cells (38). Consistent with these findings, it would be reasonable that no significant alteration of Prx-4 levels in the serum would be observed in the experiments using streptozotocin-induced diabetic rats.

LEC rats were initially identified as a mutant rat with spontaneous hepatitis and hepatoma, and thereafter were considered as a Wilson's disease model. In the liver, Prx-4 levels were slightly higher in the LEC rats compared with the control SD rats; however, no statistically significant difference was found, while this trend was inverse to the levels of serum Prx-4. Thus, it appears that the release of Prx-4 from the liver is suppressed in LEC rats. When the LEC rats were used in experiments, they did not display any symptoms of hepatitis, i.e., no apparent jaundice and no increase in serum transaminase activities (Fig. 3C and D), indicating that the lower levels of serum Prx-4 were not directly associated with inflammation. As suggested by *in vitro* studies using cultured cells, however, it appears more likely that the secretion of Prx-4 from the cells can be regulated

or affected by the redox state. Therefore, even very mild oxidative stress, which is so weak that it does not cause hepatitis, might potentially affect the secretion of Prx-4 into the blood.

The findings from this study suggest that the serum levels of Prx-4 are associated with the redox state of the liver, and therefore it is possible that this protein may be utilized as a biomarker for oxidative stress in the liver. The application of the anti-rat Prx-4 polyclonal antibody to human cell lines demonstrated no apparent reactivity (data not shown). The clinical utility of diagnosing human liver diseases will await optimizing the ELISA procedures for use in conjunction with human samples.

References

1. Halliwell B and Gutteridge JMC: Free Radicals in Biology and Medicine. 4th edition. Oxford University Press, Oxford, United Kingdom, 2007.
2. Fridovich I: Oxygen toxicity: a radical explanation. J Exp Biol 201: 1203-1209, 1998.
3. Papa S and Skulachev VP: Reactive oxygen species, mitochondria, apoptosis and aging. Mol Cell Biochem 174: 305-319, 1997.
4. Rhee SG, Kang SW, Chang TS, Jeong W and Kim K: Peroxiredoxin, a novel family of peroxidases. IUBMB Life 52: 35-41, 2001.
5. Rhee SG, Yang KS, Kang SW, Woo HA and Chang TS: Controlled elimination of intracellular H_2O_2: regulation of peroxiredoxin, catalase, and glutathione peroxidase via post-translational modification. Antioxid Redox Signal 7: 619-626, 2005.
6. Rhee SG, Chae HZ and Kim K: Peroxiredoxins: a historical overview and speculative preview of novel mechanisms and emerging concepts in cell signaling. Free Radic Biol Med 38: 1543-5152, 2005.
7. Fujii J and Ikeda Y: Advances in our understanding of peroxiredoxin, a multifunctional, mammalian redox protein. Redox Rep 7: 123-130, 2002.
8. Chang XZ, Li DQ, Hou YF, Wu J, Lu JS, Di GH, Jin W, Ou ZL, Shen ZZ and Shao ZM: Identification of the functional role of peroxiredoxin 6 in the progression of breast cancer. Breast Cancer Res 9: R76, 2007.
9. Iraqui I, Faye G, Ragu S, Masurel-Heneman A, Kolodner RD and Huang ME: Human peroxiredoxin PrxI is an orthologue of yeast Tsa1, capable of suppressing genome instability in *Saccharomyces cerevisiae*. Cancer Res 68: 1055-1063, 2008.
10. Song IS, Kim SU, Oh NS, Kim J, Yu DY, Huang SM, Kim JM, Lee DS and Kim NS: Peroxiredoxin I contributes to TRAIL resistance through suppression of redox-sensitive caspase activation in human hepatoma cells. Carcinogenesis 30: 1106-1114, 2009.
11. Neumann CA, Krause DS, Carman CV, Das S, Dubey DP, Abraham JL, Bronson RT, Fujiwara Y, Orkin SH and Van Etten RA: Essential role for the peroxiredoxin Prdx1 in erythrocyte antioxidant defence and tumour suppression. Nature 424: 561-565, 2003.
12. Fang J, Nakamura T, Cho DH, Gu Z and Lipton SA: S-nitrosylation of peroxiredoxin 2 promotes oxidative stress-induced neuronal cell death in Parkinson's disease. Proc Natl Acad Sci USA 104: 18742-18747, 2007.
13. Cha MK, Suh KH and Kim IH: Overexpression of peroxiredoxin I and thioredoxin1 in human breast carcinoma. J Exp Clin Cancer Res 28: 93, 2009.
14. Karihtala P, Mantyniemi A, Kang SW, Kinnula VL and Soini Y: Peroxiredoxins in breast carcinoma. Clin Cancer Res 9: 3418-3424, 2003.
15. Quan C, Cha EJ, Lee HL, Han KH, Lee KM and Kim WJ: Enhanced expression of peroxiredoxin I and VI correlates with development, recurrence and progression of human bladder cancer. J Urol 175: 1512-1516, 2006.
16. Lehtonen ST, Svensk AM, Soini Y, Paakko P, Hirvikoski P, Kang SW, Saily M and Kinnula VL: Peroxiredoxins, a novel protein family in lung cancer. Int J Cancer 111: 514-521, 2004.
17. Yanagawa T, Iwasa S, Ishii T, Tabuchi K, Yusa H, Onizawa K, Omura K, Harada H, Suzuki H and Yoshida H: Peroxiredoxin I expression in oral cancer: a potential new tumor marker. Cancer Lett 156: 27-35, 2000.

18. Chang JW, Jeon HB, Lee JH, Yoo JS, Chun JS, Kim JH and Yoo YJ: Augmented expression of peroxiredoxin I in lung cancer. Biochem Biophys Res Commun 289: 507-512, 2001.
19. Rhee SG, Kang SW, Jeong W, Chang TS, Yang KS and Woo HA: Intracellular messenger function of hydrogen peroxide and its regulation by peroxiredoxins. Curr Opin Cell Biol 17: 183-189, 2005.
20. Rhee SG: Cell signaling. H_2O_2, a necessary evil for cell signaling. Science 312: 1882-1883, 2006.
21. Okado-Matsumoto A, Matsumoto A, Fujii J and Taniguchi N: Peroxiredoxin IV is a secretable protein with heparin-binding properties under reduced conditions. J Biochem 127: 493-501, 2000.
22. Tavender TJ, Sheppard AM and Bulleid NJ: Peroxiredoxin IV is an endoplasmic reticulum-localized enzyme forming oligomeric complexes in human cells. Biochem J 411: 191-199, 2008.
23. Schulte J, Struck J, Bergmann A and Kohrle J: Immunolumino-metric assay for quantification of peroxiredoxin 4 in human serum. Clin Chim Acta 411: 1258-1263, 2010.
24. Tavender TJ and Bulleid NJ: Peroxiredoxin IV protects cells from oxidative stress by removing H_2O_2 produced during disulphide formation. J Cell Sci 123: 2672-2679, 2010.
25. Bertolotti M, Yim SH, Garcia-Manteiga JM, Masciarelli S, Kim YJ, Kang MH, Iuchi Y, Fujii J, Vene R, Rubartelli A, Rhee SG and Sitia R: B- to plasma-cell terminal differentiation entails oxidative stress and profound reshaping of the antioxidant responses. Antioxid Redox Signal 13: 1133-1144, 2010.
26. Ikeda Y, Ito R, Ihara H, Okada T and Fujii J: Expression of N-terminally truncated forms of rat peroxiredoxin-4 in insect cells. Protein Expr Purif 72: 1-7, 2010.
27. Matsumoto A, Okado A, Fujii T, Fujii J, Egashira M, Niikawa N and Taniguchi N: Cloning of the peroxiredoxin gene family in rats and characterization of the fourth member. FEBS Lett 443: 246-250, 1999.
28. Yoshida MC, Masuda R, Sasaki M, Takeichi N, Kobayashi H, Dempo K and Mori M: New mutation causing hereditary hepatitis in the laboratory rat. J Hered 78: 361-365, 1987.
29. Li Y, Togashi Y, Sato S, Emoto T, Kang JH, Takeichi N, Kobayashi H, Kojima Y, Une Y and Uchino J: Spontaneous hepatic copper accumulation in Long-Evans Cinnamon rats with hereditary hepatitis. A model of Wilson's disease. J Clin Invest 87: 1858-1861, 1991.
30. Wu J, Forbes JR, Chen HS and Cox DW: The LEC rat has a deletion in the copper transporting ATPase gene homologous to the Wilson disease gene. Nat Genet 7: 541–545, 1994.
31. Masuda R, Yoshida MC, Sasaki M, Dempo K and Mori M: High susceptibility to hepatocellular carcinoma development in LEC rats with hereditary hepatitis. Jpn J Cancer Res 79: 828-835, 1988.
32. Marquez-Quinones A, Cipak A, Zarkovic K, Fattel-Fazenda S, Villa-Trevino S, Waeg G, Zarkovic N and Gueraud F: HNE-protein adducts formation in different pre-carcinogenic stages of hepatitis in LEC rats. Free Radic Res 44: 119-127, 2010.
33. Samuele A, Mangiagalli A, Armentero MT, Fancellu R, Bazzini E, Vairetti M, Ferrigno A, Richelmi P, Nappi G and Blandini F: Oxidative stress and pro-apoptotic conditions in a rodent model of Wilson's disease. Biochim Biophys Acta 1741: 325-330, 2005.
34. Madhani M, Barchowsky A, Klei L, Ross CR, Jackson SK, Swartz HM and James PE: Antibacterial peptide PR-39 affects local nitric oxide and preserves tissue oxygenation in the liver during septic shock. Biochim Biophys Acta 1588: 232-240, 2002.
35. Sato H, Shiiya A, Kimata M, Maebara K, Tamba M, Sakakura Y, Makino N, Sugiyama F, Yagami K, Moriguchi T, Takahashi S and Bannai S: Redox imbalance in cystine/glutamate transporter-deficient mice. J Biol Chem 280: 37423-37429, 2005.
36. Khan N, Williams BB, Hou H, Li H and Swartz HM: Repetitive tissue pO_2 measurements by electron paramagnetic resonance oximetry: current status and future potential for experimental and clinical studies. Antioxid Redox Signal 9: 1169-1182, 2007.
37. Nagaoka Y, Iuchi, Y, Ikeda Y and Fujii J: Glutathione reductase is expressed at high levels in pancreatic islet cells. Redox Rep 9: 321-324, 2004.
38. Fujii T, Fujii J and Taniguchi N: Augmented expression of peroxiredoxin VI in rat lung and kidney after birth implies an antioxidative role. Eur J Biochem 268: 218-225, 2001.

Multiple potential regulatory sites of TLR4 activation induced by LPS as revealed by novel inhibitory human TLR4 mAbs

Hiroki Tsukamoto[1,2], Kenji Fukudome[1], Shoko Takao[1], Naoko Tsuneyoshi[1], Hideyuki Ihara[2], Yoshitaka Ikeda[2] and Masao Kimoto[1]

[1]Department of Immunology, Saga Medical School, Saga 849-8501, Japan
[2]Division of Molecular Cell Biology, Department of Biomolecular Sciences, Faculty of Medicine, Saga University, Saga 849-8501, Japan

Correspondence to: H. Tsukamoto; E-mail: tsukamoh@cc.saga-u.ac.jp

Abstract

Recognition of LPS by the toll-like receptor 4 (TLR4)/MD-2 complex is a trigger of innate immune defense against bacterial invasion. However, excessive immune activation by this receptor complex causes septic shock and autoimmunity. Manipulation of TLR4 signaling represents a potential therapy that would avoid the detrimental consequences of unnecessary immune responses. In this study, we established two novel mAbs that inhibit LPS-induced human TLR4 activation. HT52 and HT4 mAbs inhibited LPS-induced nuclear factor-κB activation in TLR4/MD-2-expressing Ba/F3-transfected cells and cytokine production and up-regulation of CD86 in the human cell line U373 and PBMCs. These inhibitory activities were stronger than that of HTA125 mAb, which we previously reported. Immunofluorescent and biochemical studies using TLR4 deletion mutants revealed that HT52 and HT4 recognized spatially distinct regions on TLR4 irrespective of MD-2 association. The HT52 and HTA125 epitopes were localized within aa 50–190, while the HT4 epitope was formed only by the full length of TLR4. In addition, we demonstrated that HT52 and HT4 failed to compete with LPS for binding to TLR4/MD-2 but inhibited LPS-induced TLR4 internalization. Inhibitory activities were not due to the interaction with the Fcγ receptor CD32. Our finding that binding of mAbs to at least two distinct regions on TLR4 inhibits LPS-dependent activation provides a novel method for manipulating TLR4 activation and also a rationale for designing drugs targeted to TLR4.

Keywords: inhibitory mAb, innate immunity, MD-2, toll-like receptor 4

Introduction

Recognition of LPS, a cell wall component of Gram-negative bacteria, by the TLR4/MD-2 complex is an important trigger of innate immune defenses against bacterial invasion (1). However, excessive immune activation by this receptor complex causes multiorgan failure due to septic shock (2, 3). In addition, TLR4 signaling has been suggested to be involved in autoimmune disease. Mice that encode multiple copies of the TLR4 gene show lupus-like autoimmune symptoms (4). In autoimmune-prone mice, TLR4 deficiency suppresses the progression of autoimmunity (5, 6). Therefore, manipulation of TLR4 signaling represents an attractive therapy that would avoid the deleterious consequences of unnecessary or improper immune responses.

TLR4 is a type I transmembrane receptor that contains repeated LRR motifs in the extracellular region and a toll/IL-1R domain in the cytoplasmic region (7). Secretory glyco-protein MD-2 is indispensable for TLR4 to recognize LPS and initiate signal transduction (8). This molecule has a large hydrophobic pocket for ligand binding and contributes to the ligand specificity of the TLR4/MD-2 complex (9, 10). Extensive studies on the interaction of TLR4, MD-2 and LPS revealed the residues critical for their interaction (11–16). Recent co-crystallographic analysis of TLR4/MD-2 (9) and TLR4/MD2/LPS (10) complexes has provided a better understanding of the molecular basis of LPS recognition. The extracellular domain of TLR4 is composed of N-terminal (aa 52–202), central (aa 203–348) and C-terminal (aa 349–582) domains, each of which consists of LRR 1–6, 7–12 and 13–22, respectively (7, 9, 10). TLR4 forms a stable complex with MD-2 at the A and B patches on the concave surface of the N-terminal and central domains (9). Five lipid chains of the lipid A moiety of LPS are completely buried inside the

hydrophobic pocket of MD-2 (10). An additional sixth lipid chain partially exposed outside this pocket interacts with the C-terminal domain of another TLR4 via hydrophobic phenylalanine residues (10, 13). Two phosphate groups of the lipid A glucosamine disaccharide, which are localized outside the pocket, also interact with positively charged residues within the central and C-terminal domains of TLR4 and MD-2 (10, 14). The resultant structural shift of the F126 loop in the MD-2-binding pocket causes the formation of a heterotetramer complex by two TLR4 and two MD-2 molecules. This is believed to initiate signal transduction by this complex (7, 10).

Pharmacological regulation of TLR4 activation has proved to be problematic. Competitive binding of a small compound in the LPS-binding pocket of MD-2 was proposed as a way of inhibiting LPS-dependent activation of TLR4. However, few synthetic LPS analogs with four lipid chains have been developed (17–19). Eritoran is currently in a suspended clinical trial. The molecular basis of their antagonism is the inability to cause a structural shift of the F126 loop in the MD-2-binding pocket due to the improper positioning of phosphate groups in lipid A (7, 10). Another possible means is blockade of the conformational change required for TLR4 signaling following LPS binding to MD-2, but the molecular basis for this allosteric regulation has not been determined.

The HTA125 mAb established by Akashi *et al.* (20) has long been used as to inhibit TLR4, while Dunn-Siegrist *et al.* (21) reported a novel inhibitory anti-TLR4 mAb, 15C1, which inhibited TLR4 by two mechanisms: binding to TLR4 and induction of an inhibitory signal by a Fc–Fcγ receptor interaction. However, how the binding of both 15C1 and HTA125 to TLR4 inhibits activation remains unknown. In this study, we established a panel of mAbs against TLR4 and TLR4/MD-2 and found that two TLR4-specific mAbs, HT52 and HT4, had potent inhibitory activities compared with HTA125. The epitopes of these mAbs were characterized by immunofluorescence and biochemical methods and compared with HTA125 and other nonfunctional mAbs. We found that HT52 has a specificity similar to that of HTA125, while HT4 recognizes a unique structure on TLR4. Furthermore, HT4 and HT52 do not compete with LPS for binding to TLR4/MD-2, whereas they inhibit LPS-induced TLR4 internalization. Inhibition was not mediated by interaction with the Fcγ receptor CD32. Based on these findings, we suggest that binding mAbs to at least two different regions of TLR4 inhibits TLR4/MD-2 activation possibly through inhibiting TLR4 internalization without competing with LPS for receptor binding. This provides valuable information in the ongoing effort to establish a new molecular basis for the design of drugs targeted to TLR4.
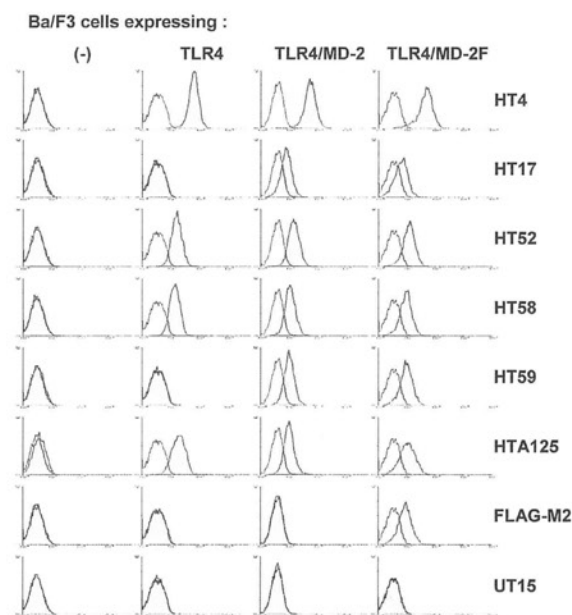
Ba/F3 cells expressing :

Fig. 1. Specificity of new anti-TLR4/MD-2 mAbs. Ba/F3 cells expressing human TLR4 alone, TLR4/MD-2 or TLR4/MD-2F were stained with the indicated mAbs (10 µg ml^{-1}) and PE-conjugated secondary antibodies and then analyzed by flow cytometry. UT15 was used for negative staining. The open histogram represents staining with PE-conjugated secondary antibody alone.

Table 1. Summary of human TLR4/MD-2 mAbs

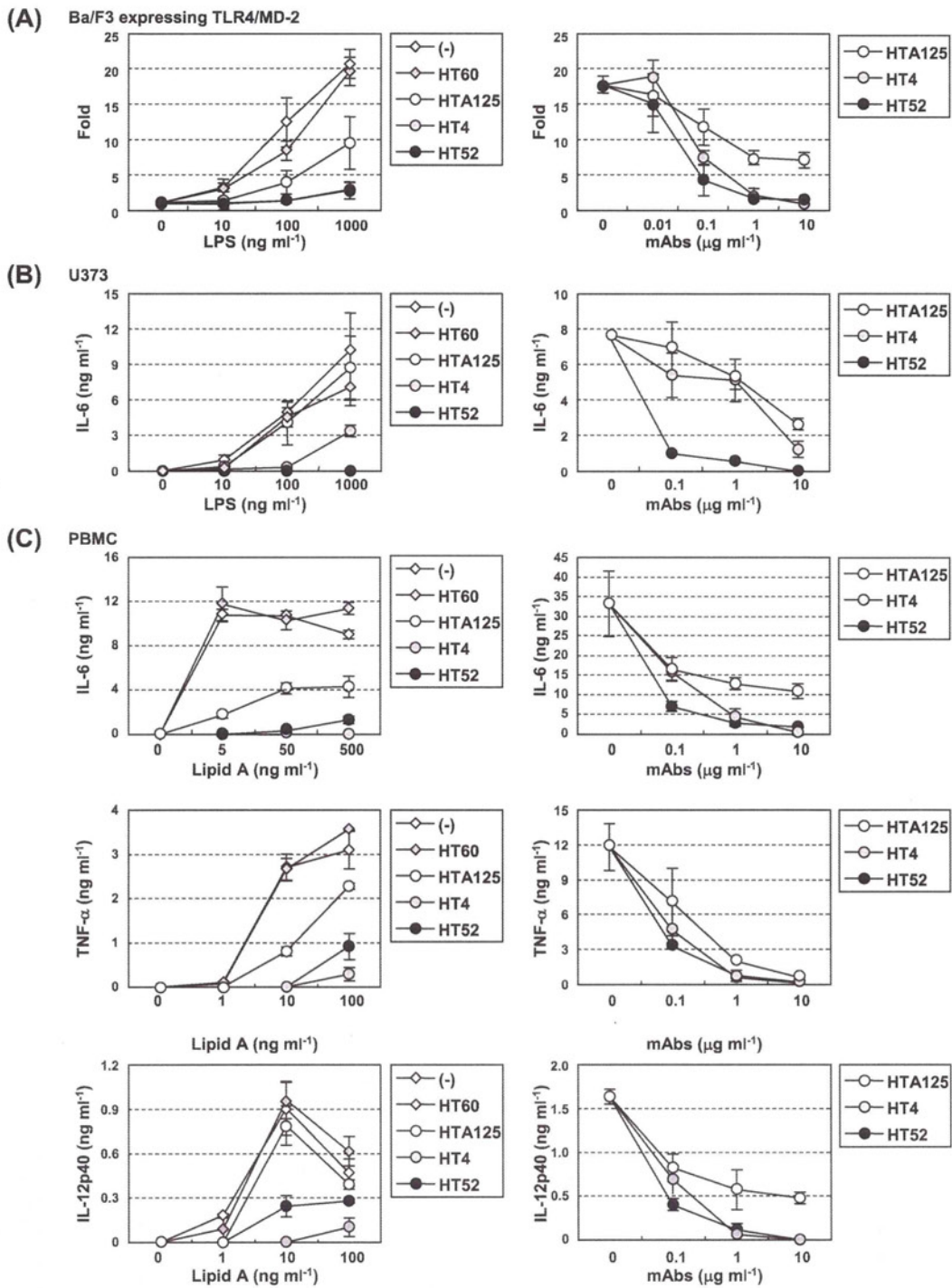| Clone	Epitope	Class	Function	Cross-blocking against Bio-mAbs					
				HT4	HT52	HTA125	HT17	HT26	HT59
HT2	TLR4	IgG1	(−)	(−)	(−)	(−)	(−)	(−	(−)
HT3	TLR4	IgG1	(−)	(−)	(−)	(−)	(−)	(−)	(−)
HT4	TLR4	IgG2b	Inhibitory	/	(−)	(−)	(−)	(−)	(−)
HT16	TLR4	IgG1	(−)	(−)	(+)	(+)	(−)	(−)	(+)
HT17	TLR4/MD-2	IgG1	(−)	(−)	(−)	(−)	/	(+)	(−)
HT26	TLR4/MD-2	IgG1	(−)	(−)	(−)	(−	(+)	/	(−)
HT41	TLR4	IgG1	(−)	(−)	(−)	(−)	(−)	(−)	(−)
HT52	TLR4	IgG1	Inhibitory	(−)	/	(+)	(−)	(−)	(−)
HT53	TLR4	IgG1	(−)	(−)	(−)	(−)	(−)	(−)	(−)
HT58	TLR4	IgG1	(−)	(−)	(+)	(+)	(−)	(−)	(+)
HT59	TLR4/MD-2	IgG1	(−)	(−)	(−)	(−)	(−)	(−)	/
HT60	TLR4	IgG1	(−)	(−)	(−)	(−)	(−)	(−)	(−)
HT68	TLR4	IgG2b	(−)	(−)	(−)	(−)	(−)	(−)	(−)
HTA125	TLR4	IgG2a	Inhibitory	(−)	(+)	/	(−)	(−)	(−)

Fig. 2. Inhibitory activities of HT4 and HT52 in cytokine production. (A) Ba/F3 cells carrying human TLR4/MD-2F and NF-κB reporter genes were stimulated with varying amounts of LPS in the presence of the indicated anti-TLR4 mAbs (10 μg ml⁻¹) (left) or stimulated with LPS (100 ng ml⁻¹) in the presence of varying amounts of mAbs (right) for 5 h. Luciferase activity was shown as the mean ± SD fold-increase against that of nonstimulated cells in triplicate cultures. (B) U373 cells were stimulated with varying amounts of LPS in the presence of mAbs (10 μg ml⁻¹) (left)
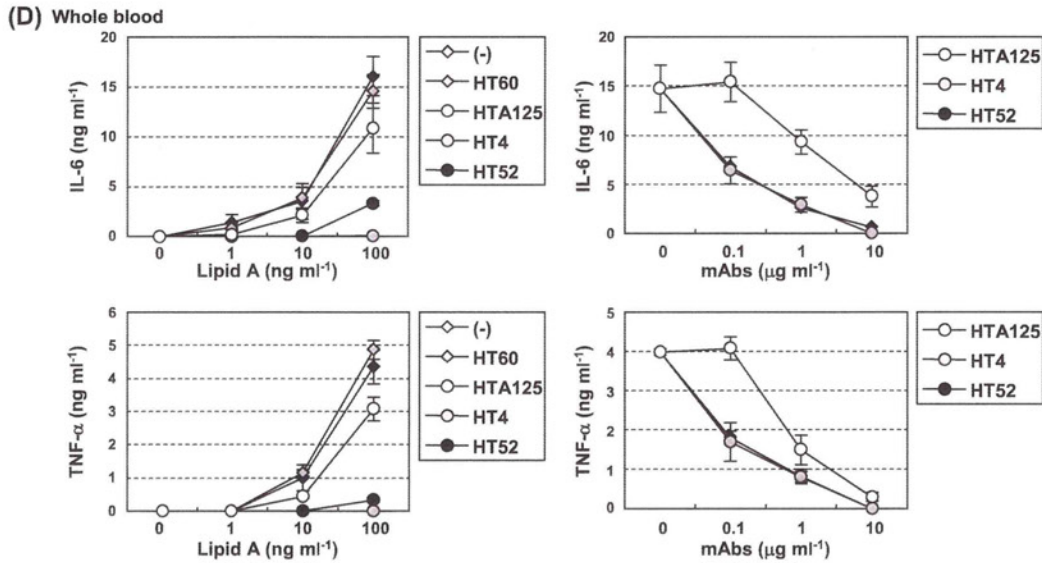
(D) Whole blood

Fig. 2. Continued

Methods

Cells

Ba/F3 and derived transfected cells were maintained in RPMI-1640 medium supplemented with 10% FCS, 100 U ml^{-1} mouse IL-3 and 50 μM β-mercaptoethanol. Mouse myeloma SP2/O cells (CRL-1581), the human embryonic kidney cell line HEK293 (CRL-1573) and the human glioblastoma cell line U373 (HTB-17) were purchased from the American Type Culture Collection (ATCC, Rockville, MD, USA). U373, HEK293 and derived transfected cells were maintained in Dulbecco's modified Eagle's medium supplemented with 10% FCS. SP2/O cells and derived hybridoma clones were maintained in RPMI-1640 supplemented with 10% FCS and 50 μM β-mercaptoethanol.

Reagents and antibodies

LPS from *Escherichia coli* ATCC 25922 was prepared as previously described (22). Lipid A was obtained from the Peptide Institute (Osaka, Japan). Mouse antihuman TLR4 mAb (HTA125) (20) and mouse anti-mouse TLR4 mAb (UT15) (23) were produced in our laboratory. Other Abs were purchased from the following companies: mouse anti-FLAG-M2 mAb and agarose-immobilized FLAG-M2 mAb from Sigma–Aldrich Co. (St Louis, MO, USA); rabbit anti-GFP antibody from Invitrogen (Carlsbad, CA, USA); mouse anti-LPS mAb WN1 222-5 from Hycult Biotechnology (Uden, The Netherlands); alkaline phosphatase-conjugated goat anti-mouse IgG from American Qualex (San Clemente, CA,

USA); alkaline phosphatase-conjugated goat anti-rabbit IgG from Kirkegaard and Perry Laboratories (Gaithersburg, MD, USA); phycoerythrin (PE)-conjugated goat anti-mouse IgG from Southern Biotechnology Associates (Birmingham, AL, USA); FITC-conjugated CD14 and PE-conjugated CD86 from Beckman Coulter (Brea, CA, USA) and PE-conjugated streptavidin from BD Biosciences (San Jose, CA, USA). Biotinylated (Bio-) antibodies were prepared using EZ-Link NHS-LC-Biotin (Pierce, Rockford, IL, USA) according to the manufacturer's instructions.

Establishment of stable HEK293 and Ba/F3-transfected cells expressing human TLR4 and MD-2

Stable HEK293-transfected clones expressing human TLR4 with or without C-terminally FLAG-tagged human MD-2 (MD-2F) were prepared as follows. A pEFBOS vector containing TLR4 and a pCAGGS1 vector containing MD-2F (16) were co-transfected into HEK293 cells using lipofectamine 2000 (Invitrogen) according to the manufacturer's instructions. Following G418 selection, stable transfected clones expressing TLR4 or TLR4/MD-2F were screened by flow cytometry using the anti-TLR4 mAb HTA125 and anti-FLAG-M2 mAb.

Stable Ba/F3-transfected cells expressing human TLR4 with or without MD-2 were prepared as follows. To obtain a tag-free human MD-2 expression vector, the full coding region of MD-2 was amplified from a pCAGGS1 vector expressing MD-2F (16) by PCR using 5'-cgcctcgagttggagatattgaatcATGT-TACC-3' and 5'-ctcgcggccgcCTAATTTGAATTAGGTTGG-3'

---

or stimulated with LPS (100 ng ml^{-1}) in the presence of varying amounts of mAbs (right) for 6 h. (C and D) PBMCs (C) or whole blood cells (D) were stimulated with varying amounts of lipid A for 6 h (IL-6, TNF-α) or 24 h (IL-12p40) in the presence of mAbs (10 μg ml^{-1}) (left) or stimulated with lipid A (10 ng ml^{-1}) in the presence of varying amounts of mAbs (right). IL-6, TNF-α and IL-12p40 levels in supernatants were determined by ELISA. Data are shown as the mean ± SD from triplicate cultures.
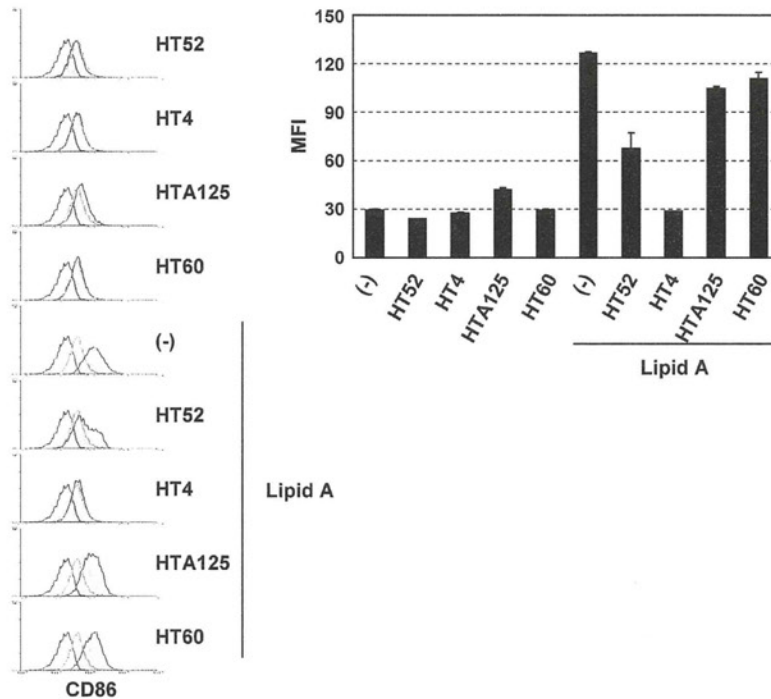
Fig. 3. Inhibitory activities of HT4 and HT52 in CD86 up-regulation Whole blood cells 1:2-diluted with RPMI medium were stimulated with lipid A (10 ng ml⁻¹) in the presence of mAbs (10 μg ml⁻¹) for 24 h. The expression level of CD86 on CD14⁺ monocytes was analyzed by flow cytometry. (Left) The open and dotted histograms represent the staining of untreated cells with PE-conjugated isotype control and CD86 mAb, respectively. (Right) MFI of CD86 was summarized. Data are shown as the mean ± SD from triplicate staining.

primers and subcloned into pCAGGS1 at *Xho*I and *Not*I sites. This was co-transfected with a pCAGGS1 expression vector containing human TLR4 (16) into Ba/F3 cells by electroporation. Following G418 selection, stable clones expressing TLR4 or TLR4/MD-2 were screened by flow cytometry using HTA125 and HT59 (established in this study, see below) mAbs, respectively. Ba/F3-transfected cells co-expressing TLR4 and MD-2F were prepared as reported previously (16) and then co-transfected with human CD14 expression vector and pBabePuro by electroporation. After puromycin selection, CD14 co-expressing stable clones were screened by flow cytometry using CD14 mAb. Full coding sequence of CD14 was subcloned into a pBluescriptKS vector (Stratagene, La Jolla, CA, USA) from an EST clone (Accession No. BC010507, Open Biosystems, Livermore, CA, USA) using *Eco*RI and *Not*I sites CD14 expression vector was prepared by subcloning *Sal*I/*Not*I-digested full coding sequence into pEFBOS vector (16) at *Xho*I and *Not*I Sites.

Establishment of mAbs against human TLR4/MD-2

TLR4⁻/⁻ mice (kindly provided by Dr S. Akira, Osaka University) on C57BL/6 genetic background were immunized intraperitoneally with 5 × 10⁷ Ba/F3-transfected cells expressing human TLR4/MD-2F as an emulsion in complete Freund's adjuvant (Difco, Lawrence, KS, USA). Ten days later, mice were boosted with 1.5 × 10⁷ of the same viable transfected cells. Three days later, spleen cells from immunized mice were fused with SP2/O myeloma cells using polyethylene glycol 1500 (Roche Applied Science, Indianapolis, IN, USA). Following HAT selection (Invitrogen), supernatants from hybridoma clones were screened by immunofluorescence staining against TLR4/MD-2F-expressing HEK293-transfected cells. Single clones were isolated by repeated limiting dilution cloning. Purified mAbs were obtained from ascitic fluids produced in SCID mice or in nude rats by caprylic acid precipitation followed by DEAE ion exchange chromatography. All animal experiments were done in accordance with the Saga Medical School guidelines for the care and treatment of animals used in experimentation.

Cell staining and flow cytometry

Cells were stained at 4°C with supernatant (1:2 dilution), 10 μg ml⁻¹ of purified mAb or 1 μg ml⁻¹ of purified Bio-mAb in staining buffer (HBSS containing 2% FCS and 0.1% azide for Ba/F3-derived cells and whole blood cells; PBS containing 3% FCS, 10 mM EDTA and 0.1% azide for HEK293-derived cells). After washing three times, cells were incubated with PE-conjugated secondary antibodies or streptavidin and subjected to flow cytometry analysis using a FACScan or FACScalibur (Becton Dickinson, Franklin Lakes, NJ, USA). In case of CD14/CD86 staining of whole blood cells, cells were stained after hemolysis.
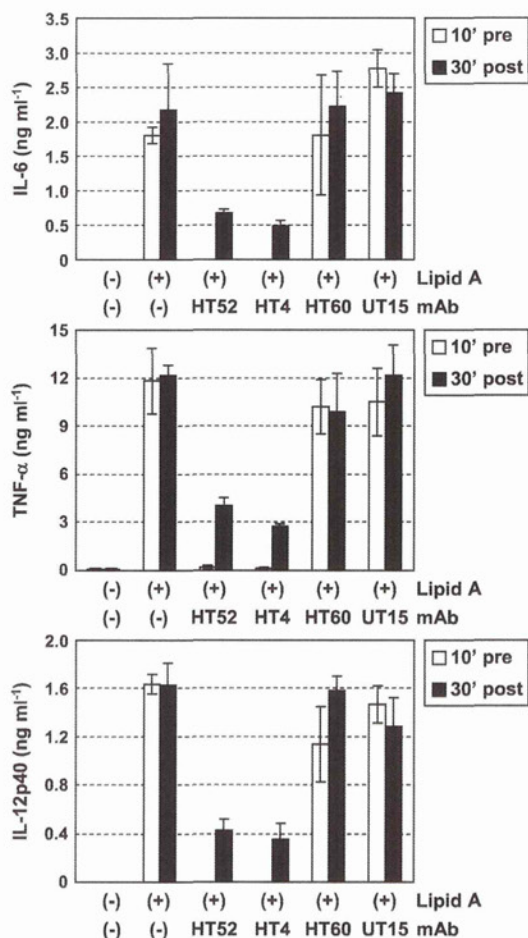
Fig. 4. Inhibition of cytokine production by post-incubation of HT4 and HT52 PBMCs were stimulated with lipid A (10 ng ml^{-1}) for 6 h (IL-6, TNF-α) or 24 h (IL-12p40). Various mAbs (10 µg ml^{-1}) were added in culture 10 min before (10′ pre, open bar) or 30 min after (30′ post, closed bar) lipid A stimulation. Cytokine levels in supernatants were determined as in Fig. 2.

For cross-blocking immunofluorescence analysis of anti-TLR4 or TLR4/MD-2 mAb, TLR4/MD-2-expressing Ba/F3-transfected cells were incubated at 4°C with 10 µg ml^{-1} of unlabeled mAb. After 5 min, 1 µg ml^{-1} Bio-mAb was added and again incubated at 4°C for 15 min. After washing three times with staining buffer, cells were incubated with PE-conjugated streptavidin for 15 min at 4°C and analyzed by flow cytometry.

For TLR4 internalization analysis, LPS-stimulated cells were washed twice by staining buffer and then stained with Bio-mAbs.

Nuclear factor-κB reporter assay in Ba/F3-transfected cells

Ten thousand Ba/F3 cells expressing TLR4/MD-2F and carrying the p55IgκBLuc nuclear factor-κB (NF-κB) reporter gene (provided by Dr K. Miyake, Tokyo University) were stimulated with LPS in a 96-well round-bottom plate in 100 µl culture medium for 5 h in the presence of anti-TLR4 mAb. Luciferase activity was measured using Steady-Glo luciferase reagent (Promega, Madison, WI, USA) and expressed as the fold-increase compared with nonstimulated cells.

Cytokine production by U373 cell lines, human PBMCs and whole blood cells

U373 cells (5 × 10^4) were cultured for 24 h in 500 µl culture medium in 48-well plates and then stimulated with LPS for 6 h in the presence of the indicated amounts of anti-TLR4 mAb. PBMCs (1 × 10^5) from healthy donors were stimulated in 100 µl culture medium in a 96-well plate with lipid A for 6 h (IL-6 and TNF-α) or 24 h (IL-12p40) in the presence of the indicated amounts of anti-TLR4 mAb. One hundred microliter of heparinized whole blood diluted with equal volume of RPMI were stimulated in a 96-well plate as well. Cytokine levels in culture supernatants and plasma were measured using ELISA kits (IL-6, eBiosciences, San Diego, CA, USA; TNF-α and IL-12p40, BioLegend, San Diego, CA). Experiments using human PBMCs were performed under the guidelines of the Ethical Committee for Research at Saga University, Faculty of Medicine.

Establishment of stable HEK293-transfected cells expressing C-terminally enhanced GFP-tagged human TLR4 (TLR4G) deletion mutants

An enhanced GFP (EGFP)-tagged full-length human TLR4 expression vector was constructed using a human TLR4/pEF-BOS vector (16), which has an *Xho*I site upstream of, and a *Bam*HI site downstream of, the TLR4 gene as cloning sites. The *Not*I site is located just downstream of *Bam*HI. The C-terminal portion of TLR4 without a stop codon was amplified from a pCAGGS1 vector containing the full coding sequence of TLR4 (16) by PCR using 5′-CCAGATATCTTCACAGAGCT-GAG-3′ and 5′-tccggatccGATAGATGTTGCTTCCTGCC-3′ primers. This PCR fragment was subcloned into the human TLR4/pEFBOS vector (16) using an *Eco*RV site on the TLR4 side and a *Bam*HI site on the vector side (both are underlined within primer sequences). Subsequently, the full coding sequence of EGFP was amplified from the pEGFP-N1 vector (Clontech, Mountain View, CA, USA) by PCR using 5′-gtcggatccATGGTGAGCAAGGGCGA-3′ and 5′-gtcgcggccgct TTACTTGTACAGCTCGTC-3′ primers and subcloned in frame into a *Bam*HI site and a *Not*I site in the vector to express the TLR4G molecule (TLR4G/pEFBOS).

The expression vectors for creating the TLR4G deletion mutants were constructed as follows. cDNA fragments coding for aa 1–49 and 1–190 of TLR4 were amplified from a TLR4/pEFBOS vector (16) by PCR using a common sense primer, 5′-ttctcaagcctcagacagtgg-3′ (which anneals vector sequences upstream of TLR4 gene) and the anti-sense primers: 5′-gaggttaacGGGGATTTTGTAGAAATTCAG-3′ for aa 1–49 or 5′-ctgtgttaacAATACTTTGAATCTTGTTGC-3′ for aa 1–190, respectively. These PCR products were subcloned into TLR4G/pEFBOS (described above) at *Xho*I (which is located downstream of the common sense primer) and *Hpa*I sites in the TLR4 gene (underlined within primer sequences). The resultant vectors, TLR4Δ50-337G/pEFBOS and TLR4Δ191-
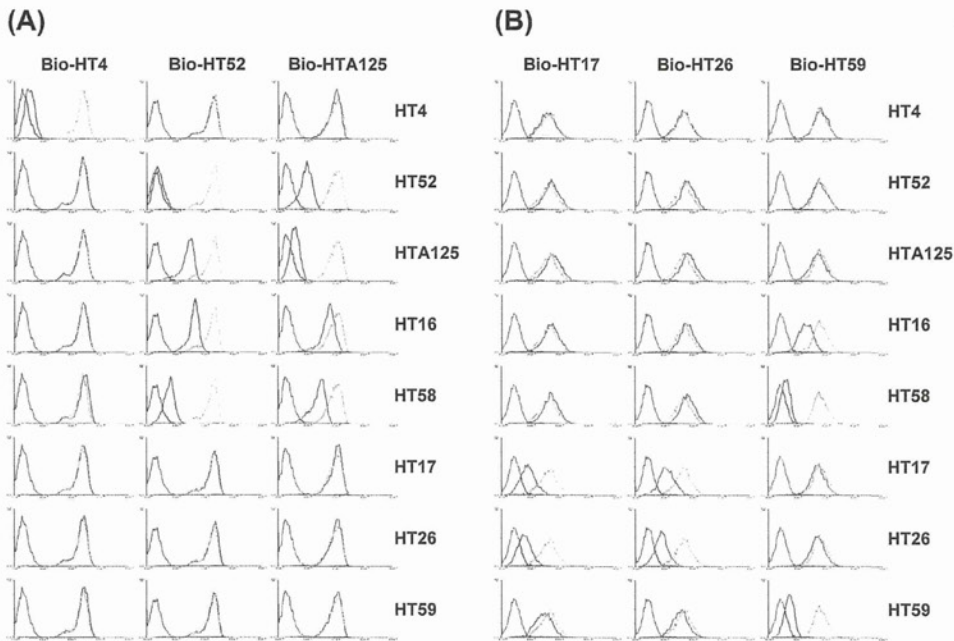
(A)

(B)

Fig. 5. Cross-blocking analysis of inhibitory mAbs. (A and B) Ba/F3 cells expressing TLR4/MD-2 were pre-incubated (shaded histogram) or not (dotted histogram) for 5 min with unlabeled mAbs (10 μg ml⁻¹) and stained with Bio-mAb (1 μg ml⁻¹) followed by PE-streptavidin. Bio-mAb immunofluorescence was analyzed by flow cytometry. The open histogram represents staining with PE-streptavidin alone.

337G/pEFBOS, express TLR4G lacking aa 50–337 (TLR4Δ50-337G) and aa 191–337 (TLR4Δ191-337G), respectively. A cDNA fragment coding for aa 580–839 of TLR4 was amplified by PCR using the sense 5′-actgttaacGACTTTGCTTG-TACTTGTG-3′ and anti-sense 5′-tccggatccGATAGATGTTGCT-TCCTGCC-3′ primers and then subcloned into TLR4G/pEFBOS (described above) at an *Hpa*I site within the TLR4 gene and a *Bam*HI site located between TLR4 and EGFP. The resultant construct, TLR4Δ340-579G/pEFBOS, expresses TLR4G lacking aa 340–579 (TLR4Δ340-579G).

TLR4G deletion pEFBOS constructs were transfected into HEK293 cells with a pBabePuro selection vector via lipofect-amine 2000. After puromycin selection, stable transfected clones were screened by EGFP fluorescence and flow cytometry.

Immunoprecipitation-western blotting

Stable HEK293-transfected cells, which were 80% confluent on a 10-cm-diameter dish, were washed twice with PBS containing 1 mM EDTA and lysed in 1 ml of 20 mM Tris buffer (pH 7.5) containing 150 mM NaCl, 1 mM EDTA, 1% Triton-X100 and 1 mM PMSF at 4°C for 20 min. After centrifugation at 15 000 × *g* for 15 min at 4°C, cell lysates were incubated with 25 μl of HT4-, HT52- or HTA125-immobilized protein G Sepharose (Amersham Biosciences, Piscataway, NJ, USA) for 2 h at 4°C with gentle rotation. As a positive control, rabbit anti-GFP polyclonal antibody directly immobilized to Affi-Gel 10 (Bio-Rad, Hercules, CA, USA) was used (24). Beads were washed three times with lysis buffer and

bound proteins were eluted by boiling in Laemmli buffer. Eluted proteins were resolved on a 7.5% SDS–PAGE gel and transferred to Immobilon-P membrane filters (Millipore Co., Bedford, MA, USA). Immunoreactivity with anti-GFP polyclonal antibody was visualized by adding alkaline phosphatase-conjugated anti-rabbit IgG and BCIP/NBT Color Development Substrate (Promega).

LPS-binding assay

LPS bound to TLR4/MD-2 was detected as reported previously (16). Briefly, 2–10 × 10⁷ Ba/F3-transfected cells expressing the TLR4/MD-2F/CD14/NF-κB reporter gene (provided by Dr K. Miyake) were pre-incubated with 10 μg ml⁻¹ HT4 or HT52 mAb for 5 min, then stimulated with LPS for 30 min. After washing with serum-free medium, cells were lysed in lysis buffer for 30 min at 4°C. After centrifugation at 15 000 × *g* for 5 min, the supernatants were incubated with FLAG-M2 mAb-immobilized agarose gels at 4°C for 2 h. Gels were washed three times with lysis buffer and boiled in Laemmli buffer. The precipitated materials were resolved by SDS–PAGE and probed with the anti-LPS mAb WN1 222-5 or FLAG-M2.

Results

Establishment of antihuman TLR4/MD-2 mAbs

By immunizing TLR4⁻/⁻ mice with Ba/F3 cells expressing human TLR4/MD-2F, we obtained nearly 3000 positive wells from four independent fusion experiments. Of these, around
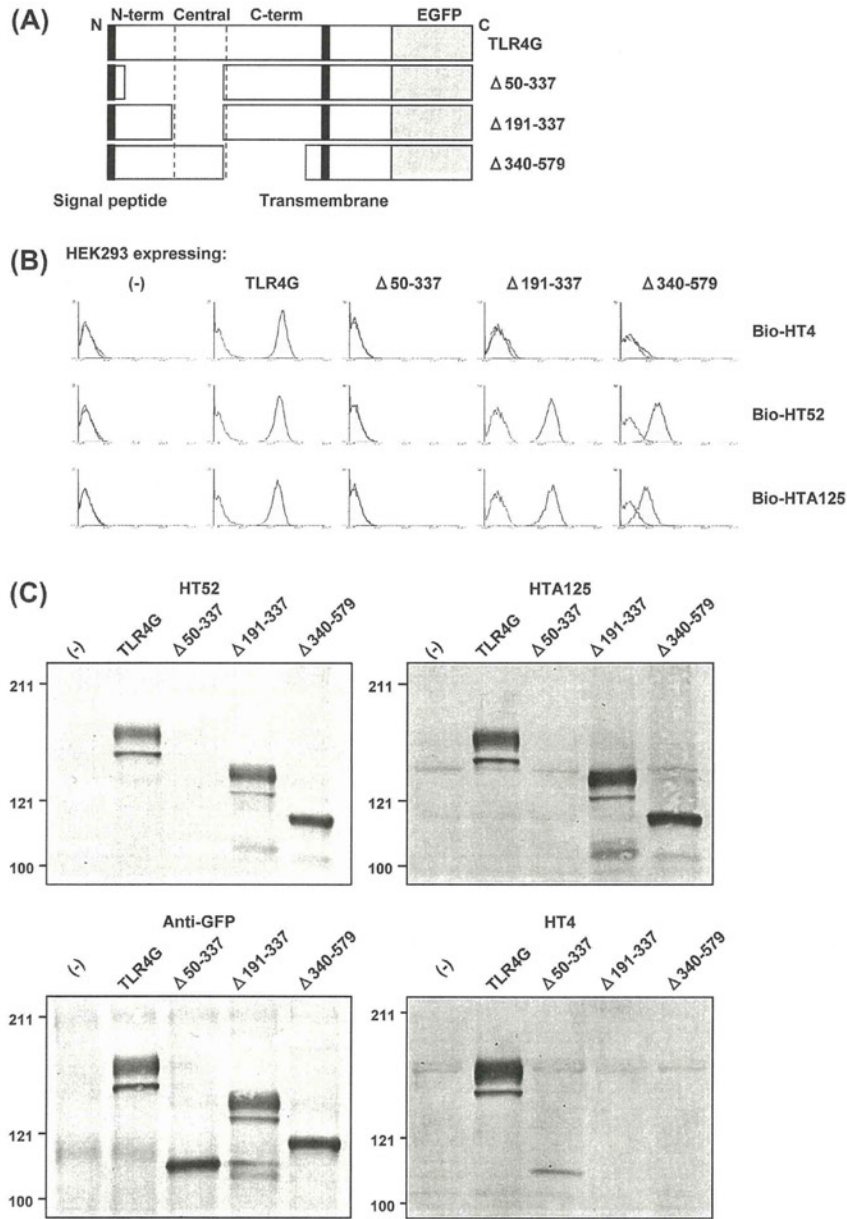
Fig. 6. Epitope analysis using a TLR4 deletion mutant. (A) Schematic description of the TLR4G deletion mutants expressed in HEK293 cells. (B) HEK293 cells expressing TLR4G or deletion mutants were stained with Bio-mAbs (2 μg ml^{-1}) followed by PE-streptavidin (shaded histogram) and then analyzed by flow cytometry. The open histogram represents staining without Bio-mAbs. (C) TLR4G or deletion mutants expressed in HEK293 cells were immunoprecipitated with the mAbs indicated and subjected to WB with anti-GFP antibody. Of note, faint signal was detected when TLR4Δ50-337G, not TLR4Δ191-337G, was precipitated by HT4 in two of two independent experiments.

70 showed positive staining against HEK293 cells expressing TLR4/MD-2F. After limiting dilution cloning, 22 independent hybridoma clones were obtained and 13 of these mAbs were successfully purified from ascitic fluids. The typical staining pattern of purified mAbs from these hybridomas against stable TLR4 and TLR4/MD-2-transfected cells are shown in Fig. 1. Most mAbs, like the established HTA125 mAb clone (20), showed reactivity against TLR4 irrespective of the presence of MD-2. Addition of an FLAG tag into MD-2 molecules did not interfere with epitope recognition, which

suggests that the epitopes for these mAbs reside on the TLR4 chain and not on the MD-2 chain. However, three mAbs (HT17, HT26 and HT59) reacted against TLR4/MD-2-, but not against TLR4-expressing cells, suggesting that the epitopes of these mAbs comprised a combinatorial structure produced by the association of TLR4 with MD-2. In addition, no mAbs reacted with mouse TLR4/MD-2-expressing Ba/F3 cells (data not shown). The characteristics of purified mAbs established in this study are summarized in Table 1.

Inhibitory antihuman TLR4 mAbs

We then examined the functional activities of antihuman TLR4/MD-2 mAbs. Supernatants from 22 independent

Fig. 7. Inhibition by HT4 and HT52 is not mediated by competition for LPS binding to TLR4/MD-2. Ba/F3-transfected cells expressing TLR4/MD-2F/CD14 and NF-κB reporter genes were pre-incubated with HT4 or HT52 (10 μg ml^{-1}) for 5 min, then stimulated with LPS (100 ng ml^{-1}) for 30 min. Cells were lysed and immunoprecipitated with FLAG-M2-immobilized agarose gels. The precipitated materials were resolved by SDS–PAGE and probed with anti-LPS mAb WNI222-5 or FLAG-M2 mAb for MD-2F as a loading control. LPS (1 ng) was run on the same gel as a positive control.

hybridoma clones were screened for agonistic and antagonistic activities using reporter Ba/F3-transfected cells carrying human TLR4/MD-2 and NF-κB reporter genes. None of the supernatants or purified mAbs showed agonistic activities, at up to a 1:2 dilution and 10 μg ml^{-1}, respectively (data not shown). In contrast, the supernatants from 2 of 22 hybridomas showed inhibitory activities when added to reporter transfected cells stimulated by LPS (data not shown). When we tested mAbs purified from these hybridomas, both HT4 and HT52 mAbs showed dose-dependent inhibition of reporter transfected cells stimulated by varying amounts of LPS (Fig. 2A). Inhibition by both of these mAbs was stronger than that of HTA125 (20). Consistent with these results, HT4 and HT52 mAbs inhibited LPS-induced IL-6 production by the human glioblastoma cell line U373 (Fig. 2B). In human PBMCs and whole blood cells, IL-6, TNF-α and IL-12p40 production after stimulation with synthetic lipid A was also blocked by the HT4 and HT52 mAbs (Fig. 2C and D). In addition to cytokine production, we further asked for inhibitory activities of these mAbs in up-regulation of co-stimulatory molecule (Fig. 3). Lipid A-induced up-regulation of CD86 in CD14$^+$ monocytes was inhibited by the incubation with HT4 and HT52. In most cases, the HT52 and HT4 mAbs showed greater inhibition than the HTA125 mAb. Considering clinical application, we further tested the effect of post-incubation with HT4 and HT52 on cytokine production. We found that these mAbs show inhibitory activities even if these were added 30 min after lipid A stimulation although the inhibition is slightly attenuated compared with pre-addition of mAbs (Fig. 4).
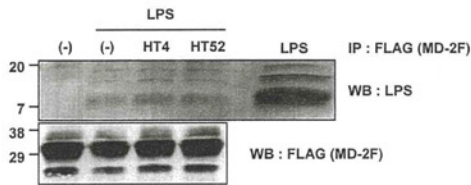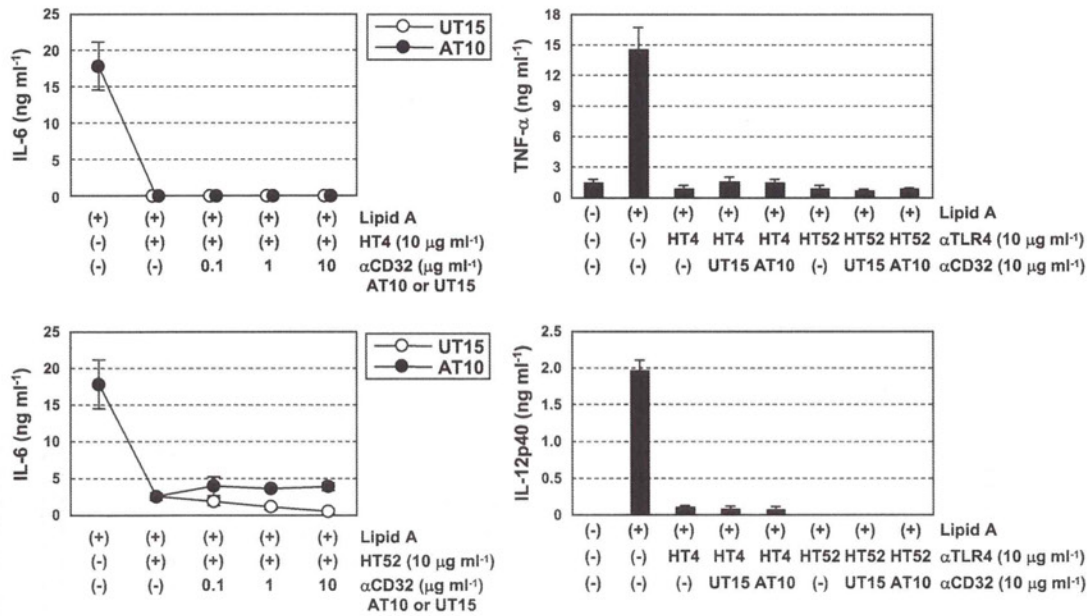

Fig. 8. HT4 and HT52 inhibition is not mediated by induction of an inhibitory signal via Fc–Fcγ receptor interaction. PBMCs were pre-incubated with indicated concentration of anti-CD32 mAb (AT10) or isotype control mAb (UT15) for 30–60 min and then stimulated with lipid A (10 ng ml^{-1}) in the presence or absence of HT4 or HT52 mAb (10 μg ml^{-1}) for 6 h (IL-6 and TNF-α) or 24 h (IL-12p40). Cytokine levels in supernatants were determined as in Fig. 2.
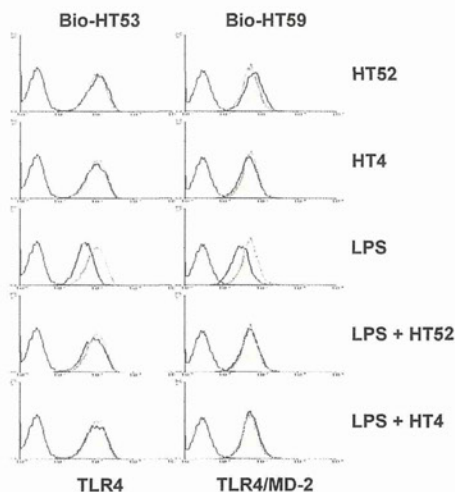
Fig. 9. HT4 and HT52 inhibit LPS-induced TLR4 internalization Ba/F3-transfected cells expressing TLR4/MD-2F/CD14 were pre-incubated with HT4 or HT52 (10 μg ml⁻¹) for 10 min, then stimulated with LPS (1 μg ml⁻¹) for 2 h. After staining with Bio-HT53 (left) and Bio-HT59 (right) followed by PE-streptavidin, surface TLR4 and TLR4/MD-2 expression levels were analyzed by flow cytometry. The open and dotted histograms represent staining of untreated cells without and with Bio-mAbs, respectively. The shaded histogram represents Bio-HT53- or Bio-HT59-specific staining of cells treated with LPS and mAbs as indicated on the right side.

Epitope analysis of inhibitory mAbs

We examined the epitopes recognized by inhibitory mAbs. We used immunofluorescent cross-blocking analysis with Ba/F3 cells expressing TLR4/MD-2. After pre-incubation with unlabeled mAb, cells were stained with Bio-mAb followed by PE-streptavidin. As shown in Fig. 5A, Bio-HT4 staining was not cross-blocked by unlabeled HT52 and HTA125. Unlabeled HT4 failed to inhibit the reaction of Bio-HT52 and Bio-HTA125 with TLR4, which suggests that the structure recognized by HT4 is spatially distinct from those recognized by HT52 or HTA125. Moreover, no other mAbs, with the exception of blocking by HT4, cross-blocked Bio-HT4 binding. This suggests that HT4 recognizes a unique structure of TLR4. In contrast, Bio-HT52 staining was cross-blocked by unlabeled HTA125, and unlabeled HT52 cross-blocked Bio-HTA125 staining. In addition to HT52 and HTA125, we found that HT16 and HT58 also showed cross-blocking of HT52 and HTA125, but not HT4, despite having no inhibitory activity against TLR4. Notably, cross-blocking analysis with Bio-HT17, HT26 and HT59, which recognize the TLR4/MD-2 complex, revealed that the HT52 and HTA125 epitopes were clearly distinguishable from those of HT16 and HT58. As shown in Fig. 5B, HT16 and HT58 cross-blocked Bio-HT59, but not Bio-HT17 and HT26 binding, although these mAbs recognize the TLR4 chain. In contrast, HT52 and HTA125 did not cross-block the three complex-type mAbs. These results indicate that the epitopes of the inhibitory mAbs HT52 and HTA125 are closely related. This subtle difference from HT16 and HT58 in terms of com-

petition with HT59 might assist in determining the inhibitory activities of HT52 and HTA125.

Next, we located the epitopes using HEK293 cells expressing TLR4 deletion mutants tagged with EGFP at the C-terminus (Fig. 6A). TLR4Δ50-337G lacks both the N-terminal and central domains in the extracellular TLR4G. TLR4GΔ191-337 and TLR4Δ340-579G lack only the central and C-terminal domains, respectively. As shown in Fig. 6B, HT52 reacted to cells with all TLR4 deletion mutants, except for TLR4Δ50-337G. Since HT52 recognized TLR4Δ191-337G, its epitope must lie between aa 50 and 190 of TLR4. In addition, HTA125 showed a similar staining pattern to HT52, suggesting that its epitope is proximal to that of HT52. In contrast, HT4 reacted only to cells expressing a complete TLR4 molecule. HT4 staining was negative for cells expressing any other deletion mutant. This indicates that the HT4 epitope differs from those of HT52 and HTA125. This is consistent with the findings of the cross-blocking experiments. The HT4 epitope may thus be composed of discontinuous sequences and is expressed only on the complete TLR4 molecule.

The lack of positive TLR4Δ50-337G staining by our mAbs, including HT52 and HTA125 (Fig. 6B, data not shown), was not due to poor expression of the constructs since these cells were EGFP-positive (data not shown). However, the negative staining may have been due to a lack of cell surface translocation. To verify the immunofluorescence results, we performed immunoprecipitation (IP)-western blotting (WB) experiments using the deletion mutants (Fig. 6C). After the lysis, TLR4G deletion mutants were immunoprecipitated with HT52- or HTA125-coupled beads and then subjected to WB with anti-GFP antibody. HT52 and HTA125 precipitated full-length TLR4G, TLR4Δ191-337G and TLR4Δ340-579G. However, both mAbs did not precipitate TLR4Δ50-337G mutants. A signal was detected from TLR4Δ50-337G when IP was performed with anti-GFP antibody. These results suggest that the HT52 and HTA125 epitope is located within aa 50–190 of TLR4. Consistent with immunofluorescence results, HT4 failed to precipitate any deletion mutants except for full-length TLR4G.

HT4 and HT52 inhibition is not mediated by competition for LPS binding to TLR4/MD-2 or by induction of an inhibitory signal via Fc–Fcγ receptor interaction

One possible mechanism of mAb inhibition of LPS-induced TLR4 activation is competition for LPS binding to MD-2. Therefore, we examined whether HT4 and HT52 compete with LPS (Fig. 7). Ba/F3 cells expressing TLR4/MD-2F were pre-incubated with either HT52 or HT4 mAb, followed by incubation with LPS. Co-precipitation of LPS with TLR4/MD-2F was examined by IP with FLAG mAb followed by WB with anti-LPS mAb. No reduction in LPS co-precipitation resulted from pre-incubation with HT4 or HT52, suggesting that competition for LPS binding to TLR4/MD-2 is not a mechanism of HT4 and HT52 inhibition.

Dunn-Siegrist *et al.* (21) demonstrated potent inhibition by antihuman TLR4 mAb 15C1. This inhibition was mediated by an antigen-antibody interaction and a concomitant induction of inhibitory signaling via Fc–Fcγ receptor IIA (CD32)

interaction on target cells. Inhibitory activity was blocked by pre-incubation with CD32 blocking mAb AT10. Therefore, we investigated the impact of AT10 on the inhibitory activities of our mAbs to reveal the contribution of CD32. As shown in Fig. 8, pre-incubation of PBMCs with AT10 did not ameliorate the inhibition of either lipid A-induced IL-6, TNF-α or IL-12p40 production by HT52 and HT4, which indicates that Fcγ receptor-mediated suppressive signaling is not the primary mechanism of HT4 and HT52 inhibition. This is also supported by our observation that U373 cells, whose IL-6 production was inhibited by the mAbs, do not express CD32, as determined by flow cytometry (data not shown).

HT4 and HT52 block TLR4 internalization induced by LPS

Another possible mechanism is inhibition of LPS-induced TLR4 internalization. To test this possibility, Ba/F3 cells expressing TLR4/MD-2F were pre-incubated with either HT52 or HT4 mAb prior to 2 h of LPS stimulation and then stained with Bio-HT53 or Bio-HT59, which recognize TLR4 chain and TLR4/MD-2 complex. Expectedly, surface TLR4 level was decreased by LPS stimulation, and its decrease was clearly prevented by HT4 and HT52 (Fig. 9). Incubation with mAbs alone did not interfere the staining with Bio-HT53 and Bio-HT59, which indicates that inhibition of TLR4 internalization is not due to epitope overlapping with HT4 and HT52. These results suggest that inhibition of TLR4 internalization is at lease in part a mechanism of inhibitory activities of HT4 and HT52.

Discussion

In this study, we developed antihuman TLR4 mAbs (HT4 and HT52) that potently inhibit the LPS-induced NF-κB activation of Ba/F3-transfected cells expressing TLR4/MD-2. They inhibited inflammatory cytokine production in U373 cells stimulated by LPS and in PBMCs and whole blood cells stimulated by lipid A. CD86 up-regulation was also blocked in CD14+ monocytes. The specificity of these mAbs, as revealed by cells transfected with TLR4 and TLR4/MD-2, indicated that both epitopes are mapped on the TLR4 chain, irrespective of the presence of MD-2. Precise epitope characterization of these mAbs and HTA125 by immunofluorescence and biochemical techniques using TLR4 deletion mutants showed that the epitopes of HT52 and HTA125 are located in a different region than that recognized by HT4. Epitopes recognized by HT52 mAb and HTA125 mAb reside between aa 50 and 190 of TLR4 molecule because these mAbs did not recognize a TLR4Δ50-337G deletion mutant but recognized both TLR4Δ191-337G and TLR4Δ340-579G mutants in both flow cytometric and biochemical analysis. The HT4 mAb epitope could be formed by discontinuous sequences of the TLR4 molecule because none of the deletion mutants reacted to HT4 in FACS analysis. Biochemical analysis of HT4 epitope showed a relatively weak signal corresponding to the expected size of TLR4Δ50-337G deletion mutant. This could result from the fact that partial sequences of HT4 epitope locate outside of this deleted portion and HT4 mAb weakly recognized such incomplete sequences.

Dunn-Siegrist *et al.* (21) reported a unique mAb, 15C1, which neutralizes LPS-stimulated activation of human PBMCs and cell lines in an Fcγ receptor-associated manner. They demonstrated that the 15C1 epitope resides in the second portion (aa 289–375) of the C-terminal domain of TLR4. This is clearly different from those of HT52 and HT4. HT52 was reactive to TLR4Δ191-337G and TLR4Δ340-579G. The HT4 epitope is present only on naive TLR4. Like HT52 and HT4, 15C1 demonstrated stronger inhibitory activity compared with HTA125. However, the mechanism underlying inhibition by 15C1 differs from that of our inhibitory mAbs because the activity of 15C1 is partially mediated by the Fcγ receptor.

Inhibition by HT52 and HT4 could not be due to blocking of LPS binding because a pull-down assay revealed that these mAbs did not compete with LPS for binding to TLR4/MD-2. Rather, the binding of inhibitory mAbs to TLR4 might confer a conformation that is refractory to the LPS-induced conformation change required for signaling. Amino acids 50–190 map to the concave surface of the N-terminal domain of extracellular TLR4. This region contains the A patch for the constitutive association of TLR4 with MD-2 (9) but is not directly involved in hydrophilic or hydrophobic interactions with LPS/MD-2 (10). According to co-crystallography, repositioning of the F126 loop in the MD-2-binding pocket enables the formation of a dimerization interface (10). The C-terminal domain of TLR4 is bent by 10° between the central and C-terminal domains (10). Therefore, the hindrance that resulted from the binding of HT52 and HT4 might have rendered TLR4/MD-2 refractory to either the induction of an active conformational change, such as TLR4 bending or the formation of a dimerization interface. Actually, several small compounds with the ability to inhibit TLR4 dimerization have been reported to inhibit murine TLR4 activation (25, 26). As another possible mechanism, we demonstrated the inhibition of LPS-induced TLR4 internalization by HT4 and HT52 mAbs. It has been reported that TLR4 signal originates both from cell surface and from endosome after internalization (27, 28). These suggest that inhibition of internalization is a part of mechanism of HT4 and HT52 inhibition. Of course, further investigation is required to uncover overall molecular mechanism, in particular, in terms of TLR4 dimerization.

The presence of multiple sites for inhibition by mAb has an important implication for manipulating TLR4 signaling. Combinatorial use of several reagents that recognize spatially different regions of TLR4 may result in more potent inhibition of LPS stimulation due to collaborative effects. Indeed, concomitant use of HT52 and HT4 was more strongly inhibitory of LPS-induced TLR4 activation than by either mAb alone (data not shown). In addition, combination with LPS analogs that compete with LPS for binding may inhibit TLR4 activation at multiple steps, i.e. LPS binding, the resulting conformational change and internalization. To our surprise, addition of HT4 or HT52 30 min after LPS stimulation was still inhibitory for cytokine production by PBMCs. Although the mechanisms for this are totally unclear, it could be possible that these inhibitory mAbs might transmit inhibitory signals by inducing nonidentified conformational changes of TLR4 after binding to their epitopes. Anyway, inhibitory effects

exerted by these mAbs after cells are activated could have a potential clinical benefit for treatment of patients with sepsis and several autoimmune inflammatory diseases.

In conclusion, we revealed the presence of at least two potential sites on TLR4 that regulate LPS-induced activation. Further analysis of the TLR4 structures that are recognized by these inhibitory mAbs would provide fundamental information for developing a novel strategy to manipulate TLR4 activation and a molecular basis for designing TLR4-targeted drugs. We also hope that HT52 and HT4 are useful for developing clinically applicable inhibitory TLR4 mAbs.

Funding

Acknowledgements

References

1 Akira, S., Uematsu, S. and Takeuchi, O. 2006. Pathogen recognition and innate immunity. *Cell* 124:783.
2 Hennessy, E. J., Parker, A. E. and O'Neill, L. A. 2010. Targeting Toll-like receptors: emerging therapeutics? *Nat. Rev. Drug Discov.* 9:293.
3 Hoshino, K., Takeuchi, O., Kawai, T. *et al.* 1999. Toll-like receptor 4 (TLR4)-deficient mice are hyporesponsive to lipopolysaccharide: evidence for TLR4 as the Lps gene product. *J. Immunol.* 162:3749.
4 Liu, B., Yang, Y., Dai, J. *et al.* 2006. TLR4 up-regulation at protein or gene level is pathogenic for lupus-like autoimmune disease. *J. Immunol.* 177:6880.
5 Lartigue, A., Colliou, N., Calbo, S. *et al.* 2009. Critical role of TLR2 and TLR4 in autoantibody production and glomerulonephritis in lpr mutation-induced mouse lupus. *J. Immunol.* 183:6207.
6 Choe, J. Y., Crain, B., Wu, S. R. and Corr, M. 2003. Interleukin 1 receptor dependence of serum transferred arthritis can be circumvented by toll-like receptor 4 signaling. *J. Exp. Med.* 197:537.
7 Kang, J. Y. and Lee, J. O. 2011. Structural biology of the toll-like receptor family. *Annu. Rev. Biochem.* 80:917.
8 Nagai, Y., Akashi, S., Nagafuku, M. *et al.* 2002. Essential role of MD-2 in LPS responsiveness and TLR4 distribution. *Nat. Immunol.* 3:667.
9 Kim, H. M., Park, B. S., Kim, J. I. *et al.* 2007. Crystal structure of the TLR4-MD-2 complex with bound endotoxin antagonist Eritoran. *Cell* 130:906.
10 Park, B. S., Song, D. H., Kim, H. M., Choi, B. S., Lee, H. and Lee, J. O. 2009. The structural basis of lipopolysaccharide recognition by the TLR4-MD-2 complex. *Nature* 458:1191.
11 da Silva Correia, J. and Ulevitch, R. J. 2002. MD-2 and TLR4 N-linked glycosylations are important for a functional lipopolysaccharide receptor. *J. Biol. Chem.* 277:1845.
12 Fujimoto, T., Yamazaki, S., Eto-Kimura, A., Takeshige, K. and Muta, T. 2004. The amino-terminal region of toll-like receptor 4 is essential for binding to MD-2 and receptor translocation to the cell surface. *J. Biol. Chem.* 279:47431.
13 Resman, N., Vasl, J., Oblak, A. *et al.* 2009. Essential roles of hydrophobic residues in both MD-2 and toll-like receptor 4 in activation by endotoxin. *J. Biol. Chem.* 284:15052.
14 Meng, J., Lien, E. and Golenbock, D. T. 2010. MD-2-mediated ionic interactions between lipid A and TLR4 are essential for receptor activation. *J. Biol. Chem.* 285:8695.
15 Nishitani, C., Mitsuzawa, H., Sano, H., Shimizu, T., Matsushima, N. and Kuroki, Y. 2006. Toll-like receptor 4 region Glu24-Lys47 is a site for MD-2 binding: importance of CYS29 and CYS40. *J. Biol. Chem.* 281:38322.
16 Tsuneyoshi, N., Fukudome, K., Kohara, J. *et al.* 2005. The functional and structural properties of MD-2 required for lipopolysaccharide binding are absent in MD-1. *J. Immunol.* 174:340.
17 Mullarkey, M., Rose, J. R., Bristol, J. *et al.* 2003. Inhibition of endotoxin response by e5564, a novel Toll-like receptor 4-directed endotoxin antagonist. *J. Pharmacol. Exp. Ther.* 304:1093.
18 Christ, W. J., Asano, O., Robidoux, A. L. *et al.* 1995. E5531, a pure endotoxin antagonist of high potency. *Science* 268:80.
19 Kovach, N. L., Yee, E., Munford, R. S., Raetz, C. R. and Harlan, J. M. 1990. Lipid IVA inhibits synthesis and release of tumor necrosis factor induced by lipopolysaccharide in human whole blood ex vivo. *J. Exp. Med.* 172:77.
20 Akashi, S., Ogata, H., Kirikae, F. *et al.* 2000. Regulatory roles for CD14 and phosphatidylinositol in the signaling via toll-like receptor 4-MD-2. *Biochem. Biophys. Res. Commun.* 268:172.
21 Dunn-Siegrist, I., Leger, O., Daubeuf, B. *et al.* 2007. Pivotal involvement of Fcγ receptor IIA in the neutralization of lipopolysaccharide signaling via a potent novel anti-TLR4 monoclonal antibody 15C1. *J. Biol. Chem.* 282:34817.
22 Tsuneyoshi, N., Kohara, J., Bahrun, U. *et al.* 2006. Penta-acylated lipopolisaccharide binds to murine MD-2 but does not induce the oligomerization of TLR4 required for signal transduction. *Cell. Immunol.* 244:57.
23 Bahrun, U., Kimoto, M., Tsukamoto, H., Tsuneyoshi, N., Kohara, J. and Fukudome, K. 2007. Preparation and characterization of agonistic monoclonal antibodies against Toll-like receptor 4-MD-2 complex. *Hybridoma (Larchmt)* 26:393.
24 Tsukamoto, H., Fukudome, K., Takao, S., Tsuneyoshi, N. and Kimoto, M. 2010. Lipopolysaccharide-binding protein-mediated Toll-like receptor 4 dimerization enables rapid signal transduction against lipopolysaccharide stimulation on membrane-associated CD14-expressing cells. *Int. Immunol.* 22:271.
25 Park, S. J., Kang, S. H., Kang, Y. K. *et al.* 2011. Inhibition of homodimerization of toll-like receptor 4 by 4-oxo-4-(2-oxo-oxazolidin-3-yl)-but-2-enoic acid ethyl ester. *Int. Immunopharmacol.* 11:19.
26 Youn, H. S., Saitoh, S. I., Miyake, K. and Hwang, D. H. 2006. Inhibition of homodimerization of Toll-like receptor 4 by curcumin. *Biochem. Pharmacol.* 72:62.
27 Zanoni, I., Ostuni, R., Marek, L. R. *et al.* 2011. CD14 controls the LPS-induced endocytosis of Toll-like receptor 4. *Cell* 147:868.
28 Kagan, J. C., Su, T., Horng, T., Chow, A., Akira, S. and Medzhitov, R. 2008. TRAM couples endocytosis of Toll-like receptor 4 to the induction of interferon-beta. *Nat. Immunol.* 9:361.

５． 資料　検診で配布した説明書など

新骨検診法試験への参加のおねがい

骨粗鬆症検診受検のみなさまへ

　５０歳を越えると**骨粗しょう症**による骨折が増加します。とくに足の付け根の骨折件数は年間約１５万件にもなります。骨折が原因でそのまま**寝たきり**になると平均７年で死亡するというデータもあります。国は骨折予防のための**骨粗しょう症検診**（骨検診）を推奨しておりますが、実際に検診を受けているひとはまだまだ少ないのが現状です。

　私たちは、健康診断のときに、いっしょに骨の検診もできるような簡便で安価な検査法を開発しましたが、さらに性能を向上させる目的で、今年度から、体組成検査等を組み合わせた検査法の性能試験に参加をお願いしております（４５歳以上７５歳未満）。

　参加をご希望の方は、同封されている、試験の目的や方法についての**説明書**をよくお読みください。検査は、保健センターでの体組成検査と、希望者のみ、あいち健康プラザにおいて、早朝尿の提出・大腿骨・腰椎の骨密度測定、血液検査等、健康状態を総合的にチェックし、改善ポイントをみつける健康度評価（Bコース）を実施致します。なお、検査に係る費用はいっさい発生いたしません。

　試験に関する説明について十分ご理解頂き、参加に同意頂けるときは、同封の**同意書**にご署名と連絡先（結果の送付先）を記入の上、骨粗しょう症検診当日にご持参ください。

　ご協力、よろしくお願いいたします。

<div style="text-align: right">

厚生労働省長寿科学総合研究事業
研究班代表
国立長寿医療研究センター　新飯田俊平

</div>

骨粗しょう症の新しい検査法試験について

　わが国の骨粗しょう症検診（骨検診）の受診率はわずか５％です。私たちは少しでも多くの方に骨検診を受けてもらえるように、低コストで簡便な検査法を開発しましたが、今回、この検査方法の性能を向上させる目的で、筋肉量や体脂肪などの体組成の数値や問診票の点数などを組み合わせた方法で検診の効果を評価することになりました。以下に、今回の試験の目的、方法、研究対象者などについて説明いたします。

１．試験の目的

　　今回実施する検査方法で、骨量減少症または骨粗鬆症の人をどれくらいの精度で見つけることが出来るかを評価することが目的です。

２．検査対象者の抽出と対象年齢

・　東浦町の骨粗鬆症検診の申込者を対象とさせて頂いております。

・　本年度の尿検診は**45歳以上**とさせて頂きます。

３．どんな検査をするのか

　　尿中に存在する、γ‐グルタミルトランスペプチダーゼ（γ-GTP）という酵素の活性値を測定します。この値が高いほど骨吸収が亢進（骨が減る）している状態にあると考えられます。

４．試験の方法

・　検査は、**あいち健康プラザでの検査当日の早朝の尿**を用いて測定します。**起床後に採尿キットで尿をびんの線のある位置まで**入れ、検診会場までお持ちください。（採尿キットは、保健センターで骨密度検査後、あいち健康プラザでの検査希望者にお渡しいたします。）

・　この検査方法を評価するために、同じ尿を使っての既存の骨代謝マーカーを一緒に測定する場合があります。

・　東浦町で実施する骨密度検査の結果も評価に活用させて頂きます。

・　骨折リスク判定のための<u>問診票（同封の白い紙）</u>の記入をお願いします。

５．結果の通知方法

検査結果は本人に直接封書にて通知いたします。**骨吸収が亢進状態**にある方にはその後の医療機関受診の有無などを調査するために電話等で確認させて頂くことがありますのでご協力をお願い致します。

６．健康上の被害と補償について

　　採尿したものの一部を使用させていただくだけですので健康を害するものではありません。

７．個人情報の保護について

　　この試験で得られた結果は、厚生労働省への提出資料として使用するほか、医学会、医学雑誌などで発表することはありますが、被験者様のお名前などの個人情報は一切わからないようにいたしますので、プライバシーは完全に守られます。